Solution-Processable Hosts Constructed by Carbazole/PO Substituted Tetraphenylsilanes for Efficient Blue Electrophosphorescent Devices

He Liu, Qing Bai, Liang Yao, Dehua Hu, Xiangyang Tang, Fangzhong Shen, Huanhuan Zhang, Yu Gao, Ping Lu, Bing Yang, and Yuguang Ma*

Two new solution-processable wide bandgap materials, bis(4-((4-(9-H-carbazol-9-yl)phenyl)diphenylsilyl)phenyl)(phenyl)phosphine oxide (CS_2PO) and bis(4-((4-(9-H-(3,9′-bicarbazol)-9-yl)phenyl)diphenylsilyl)phenyl)(phenyl) phosphine oxide (DCS_2PO), have been developed for blue phosphorescent light-emitting diodes by coupling an electron-donating carbazole moiety and an electron-accepting PO unit together via double-silicon bridges. Both of them have been characterized as having high glass transition temperatures of 159–199 °C, good solubility in common organic solvent (20 mg mL^{-1}), wide optical gap (3.37–3.55 eV) and high triplet energy levels (2.97–3.04 eV). As compared with their corresponding single-silicon bridged compounds, this design strategy of extending molecular structure endows CS_2PO and DCS_2PO with higher thermal stability, better solution processability and more stable film morphology without lowering their triplet energies. As a result, DCS_2PO/FIrpic doped blue phosphorescent device fabricated by spin-coating method shows the best electroluminescent performance with a maximum current efficiency of 26.5 cd A^{-1}, a maximum power efficiency of 8.66 lm W^{-1}, and a maximum external quantum efficiency of 13.6%, which is one of the highest efficiencies among small molecular devices with the same deposition process and device configuration.

1. Introduction

Organic wide bandgap materials which emit violet or ultraviolet (UV) light are of great importance owing to their potential applications in UV detectors,[1] laser diodes[2] and high density information storage devices.[3] They also show enormous values in organic light emitting diodes to be used as host materials for fluorescent and phosphorescent dyes to generate light of all colors by energy transfer process.[4,5] Phosphorescent organic light emitting diodes (PhOLEDs) which can theoretically achieve 100% internal quantum efficiency by harvesting both singlet and triplet excitons have been devoted tremendous efforts in the past decades.[6] Most successful cases are the red and green electrophosphorescent devices,[7,8] while the blue one is still lagging behind in terms of efficiency and stability. In doping blue PhOLEDs, the suitable wide bandgap host material plays a crucial role for the device performance. Recently, some small molecule/FIrpic (iridium(III) bis(4,6-(difluorophenyl)-pyridinato-*N,C2′*) picolinate) PhOLEDs have achieved high efficiencies through vacuum-deposited method.[9] However, high cost, complicated device structures, difficulties in host/guest ratio control and unavoidable waste of a large amount of organic materials have prevented this method from further application. For low cost general light application or display on large area, a simple solution approach, such as spin-coating and inkjet printing, is believed to be an alternative way superior to vacuum deposition.[10] Taking the advantages of high purity and certain molecular structure, solution-processable wide bandgap hosts for blue PhOLEDs are significantly needed to be developed.

Wide bandgap small molecules usually show poor thermal stability, tendency to crystallize, inferior film forming ability and difficulty in carrier injection due to the low molecular weights and intrinsic wide energy gap. Thus, the high T_g, good film-forming ability, bipolar carriers injection, and high triplet energy levels to prevent the energy back transfer[5a] are the key issues to be taken into consideration for suitable hosts. Recently, tetraphenylsilane (TPS) has emerged as an ideal group for constructing organic wide bandgap materials.[4a,11–13] Firstly, the δ-π* silicon can effectively confine the conjugation length of molecules to obtain the wide bandgap. Secondly, the natural twisted tetrahedron geometry of tetraphenylsilane can effectively prevent the intermolecular interaction in solid state and thus enables formation of smooth and stable amorphous films. Thirdly, from the point of synthetic chemistry, it is possible to introduce hole and electron-injecting substituents to tetraphenylsilane

Dr. H. Liu, Q. Bai, Dr. L. Yao, Dr. D. Hu, X. Tang, Dr. F. Shen, H. Zhang, Y. Gao, Prof. P. Lu, Prof. B. Yang, Prof. Y. Ma
State Key Laboratory of Supramolecular Structure and Materials
Jilin University
Changchun 130012, PR China
E-mail: lup@jlu.edu.cn

DOI: 10.1002/adfm.201401183

through classical reactions. In our recent work, we have developed a series of silicon-cored wide bandgap molecules, which contains p-type carbazole units and n-type phosphine oxide (PO) units with different ratios and linking fashions.[14] Blue PhOLEDs with a high EQE of 27.5% and a maximum current efficiency of 49.4 cd A^{-1} were realized in the vacuum-deposited doped device. However, the poor solution processability is not suitable for the fabrication of low cost spin-coating devices. To further develop the solution-processable host materials in this system, here, we try to increase the solubility of materials by extending the molecular structure through a double-silicon bridge taking the full advantage of the flexible silicon-carbon bond. Two new wide bandgap molecules named as bis(4-((4-(9-H-carbazol-9-yl)phenyl)diphenylsilyl)phenyl)(phenyl)phosphine oxide (CS_2PO) and bis(4-((4-(9-H-(3,9′-bicarbazol)-9-yl)phenyl) diphenylsilyl)phenyl)(phenyl)phosphine oxide (DCS_2PO) are thus designed and synthesized. The thermal stability, film morphology, theoretical calculations, electrochemistry behaviors, photophysical and electroluminescent properties of these new compounds are systematically investigated. As compared with their corresponding single-silicon bridged compounds 4-diphenylphosphrineoxide-4′-9H-carbazole-9-yl-tetraphenylsilane (CSPO) and 4-diphenylphosphrineoxide-4′-[3-(9H-carbozale-9-yl)-9H-carbazole-9-yl]-tetraphenylsilane (DCSPO), the solubility, thermal stability and film-forming ability are greatly improved in CS_2PO and DCS_2PO, while the bipolar transporting nature, high singlet and triplet energy levels are maintained. The solution-processed DCS_2PO/FIrpic device has achieved a a maximum current efficiency of 26.5 cd A^{-1} and a maximum external quantum efficiency of 13.6%. The results clearly demonstrate that the new wide bandgap material presents the potentiality as suitable host for solution-processed high-efficiency blue PhOLEDs.

2. Results and Discussion

2.1. Synthesis and Characterization

The chemical structures of CSPO, DCSPO CS_2PO and DCS_2PO are shown in **Scheme 1**. The detailed synthetic route is given in supporting information (Scheme S1). CS_2PO and DCS_2PO both have a double silicon skeleton. In our previous work, DCSPO with carbazole dimer/PO (2:1) substitutents showed more balanced charge injection and transport properties.[14] Here, the ratio of p-type carbazole and n-type PO units was designed as 2:1 for CS_2PO and 4:1 for DCS_2PO to ensure the balanced carrier flux since no hole-transporting layer was applied between hole-injecting layer (usually PEDOT/PSS) and emitting layer (EML) in spin-coating devices. All these materials were synthesized through classical Ullmann reaction between respective substituted carbazoles and phosphine oxide monomers. The compounds were fully characterized by ^1H NMR and ^{13}C NMR spectroscopy, mass spectrometry, elemental analysis and corresponded well with their expected structures. In addition, CS_2PO and DCS_2PO show good solubility (20 mg mL^{-1}) in common organic solvent such as toluene, chloroform, chlorobenene and tetrahydrofuran.

2.2. Thermal Properties

Differential scanning calorimetry (DSC) and thermal gravimetric analysis (TGA) were performed to investigate the thermal stability of these compounds (**Figure 1** and Figure S1). It is found that double-silicon bridged compounds show better thermal stability than the single-silicon bridged ones. The DSC traces of CS_2PO displays a distinct glass transition temperature (T_g) of 159 °C, which is 49 °C higher than that of CSPO. The T_g of DCS_2PO is found at 199 °C, which is 59 °C higher than that of DCSPO. All these facts prove that T_g can be greatly increased by the introduction of one more silicon center. TGA measurement reveals that the decomposition temperatures (T_d) are at 420, 421, 485 and 521 °C for CSPO, DCSPO, CS_2PO and DCS_2PO, respectively. The increase in T_d is proportional to the increase in molecular weight. The TGA and DSC characterizations demonstrate that DCS_2PO displays the best thermal stability which is beneficial for the OLED application.

2.3. Morphology

The morphological stability of the solution-processed films of the four compounds doped with 15 wt% FIrpic was estimated by atomic force microscopy (AFM). The images are given in **Figure 2**. All the films show smooth surface with small

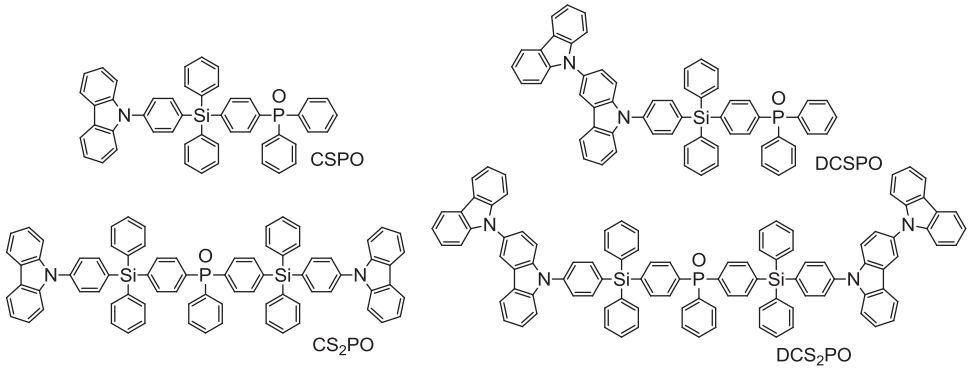

Scheme 1. The chemical structures of CSPO, DCSPO, CS_2PO and DCS_2PO.

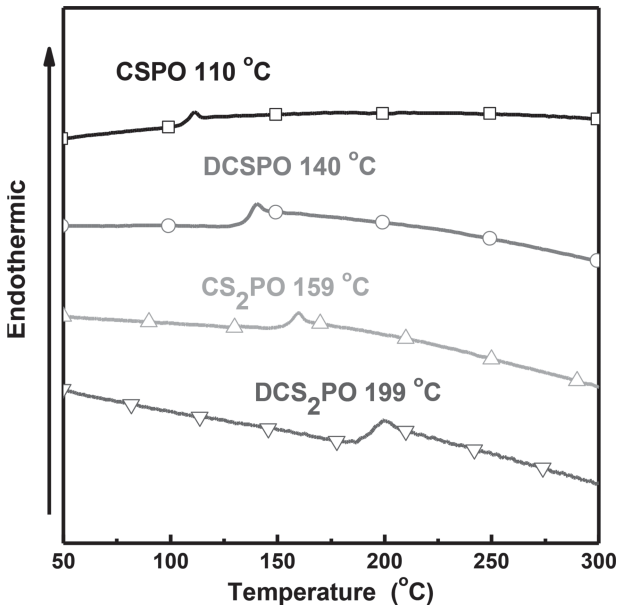

Figure 1. DSC curves for CSPO, DCSPO, CS_2PO and DCS_2PO at heating rate of 10 K min^{-1} under nitrogen.

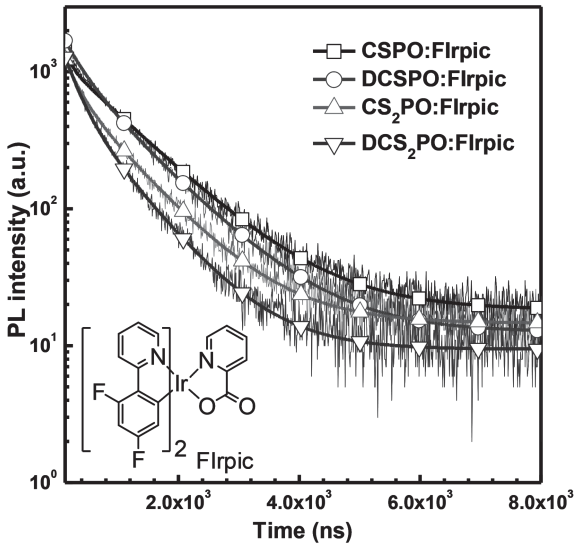

Figure 3. Room temperature transient PL decay of solution-processed CSPO, DCSPO, CS_2PO and DCS_2PO films doped with 15 wt% FIrpic (excitation wavelength = 360 nm, detection wavelength = 475 nm).

root-means-square (RMS) values ranged from 0.33 to 0.38 nm before annealing, and 0.29 to 0.36 nm after annealing. The results suggest that twisted tetrahedron geometry of silicon and flexibility of carbon-silicon bond could provide a homogeneous morphology of spin-coating films. All the films remain almost unchanged after thermal annealing indicating the possibility to keep uniform films throughout the device fabrication process.

Figure 3 shows the transient photoluminescent (PL) decay of FIrpic doped films of the four host materials. All of them present monoexponential decays indicative of the well confinement of excitons on FIrpic. As shown in **Table 1**, DCS_2PO doping film exhibits the shortest lifetime of 0.79 μs, which suggests the triplet-triplet annihilation may be reduced in its doped film which is favorable for its application in blue PhOLEDs.

2.4. Photophysical Properties

The normalized optical absorption spectra in dilute CH_2Cl_2 are shown in **Figure 4** and Figure S2. All the four compounds display the similar absorption spectra because of the same building fragments. The maximum absorption peak at 293 nm and the absorption band from 324 to 344 nm are attributed to the π-π^* transition of the carbazole.[15] The optical bandgaps (E_g) calculated from the absorption edge for CSPO, CS_2PO, DCSPO, DCS_2PO are as wide as 3.56, 3.55, 3.38 and 3.37 eV, respectively.

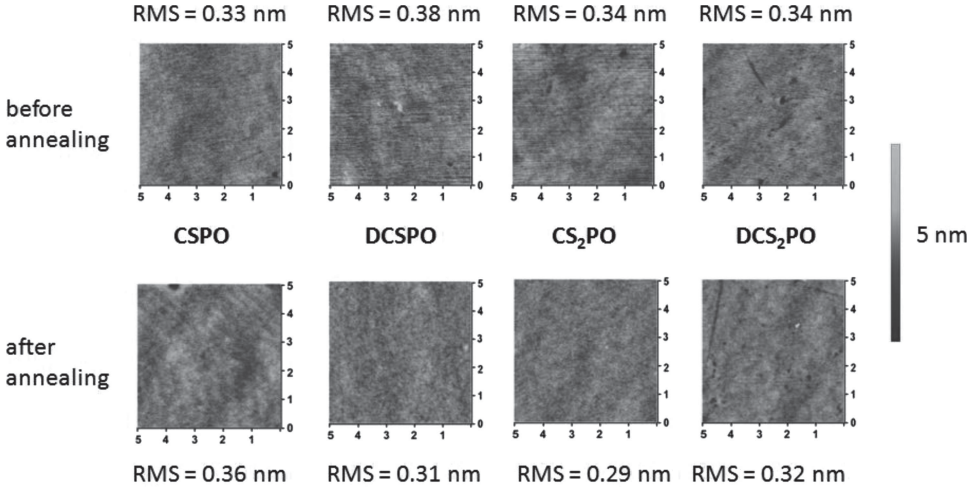

Figure 2. AFM images (5 μm × 5 μm) of solution-processed CSPO, DCSPO, CS_2PO and DCS_2PO films doped with 15 wt% FIrpic from chlorobenzene (concentration = 20 mg mL^{-1}) before and after annealing at 110 °C for 1 h under ambient atmosphere.

Table 1. Detailed optical and thermal properties of CSPO, DCSPO, CS_2PO and DCS_2PO.

Compounds	Abs_{max} [nm]	PL_{max} [nm]	E_g[a)] [eV]	E_T [eV]	τ [μs]	T_g [°C]	T_d [°C]
CSPO	294,326,341	347,362	3.56	3.04	1.03	110	420
DCSPO	294,342	379	3.36	2.97	0.98	140	420
CS_2PO	293 325,342	347,363	3.55	3.04	0.89	159	485
DCS_2PO	295,342	375	3.37	2.97	0.79	199	521

[a)]calculated from the absorption edge.

The four compounds all emit in the violet or ultraviolet region. CSPO and CS_2PO present quite similar emission spectra peaking at 347 and 362 nm, respectively, which are derived from the group of carbazolesilanes as revealed previously.[14] The same phenomenon is also observed in the emission spectra of DCSPO and DCS_2PO. Both of them exhibit the same emission spectra peaking at 379 nm. As compared with CSPO and CS_2PO, the further red-shift of the signal for the DCSPO and DCS_2PO is ascribed to their enlarged conjugation through the substituted dimer carbazole unit. No emission band at longer wavelength is observed demonstrating the tetrahedral geometry can effectively interrupt the interaction between donor and acceptor in these compounds. The results depict that the high singlet levels of CS_2PO and DCS_2PO are maintained after introducing double-silicon bridge, which is consistent with our molecular design. The photophysical data is summarized in Table 1.

The phosphorescent spectra of the four compounds were measured in frozen CH_2Cl_2 at 77 K. The triplet energy levels (E_T) were estimated to be 3.04 eV for CSPO and CS_2PO, and 2.97 eV for DCSPO and DCS_2PO from their respective highest energy vibronic peak. It can be seen that the E_Ts are all higher than that of blue phosphorescent dye FIrpic (E_T = 2.67 eV), which means that they could be used as suitable hosts to effectively confine the excitons on guest of FIrpic in doping system. The same triplet energy levels further prove that π-conjugation in the whole molecule remains unchanged when the molecular structure is extended by double-silicon bridge.

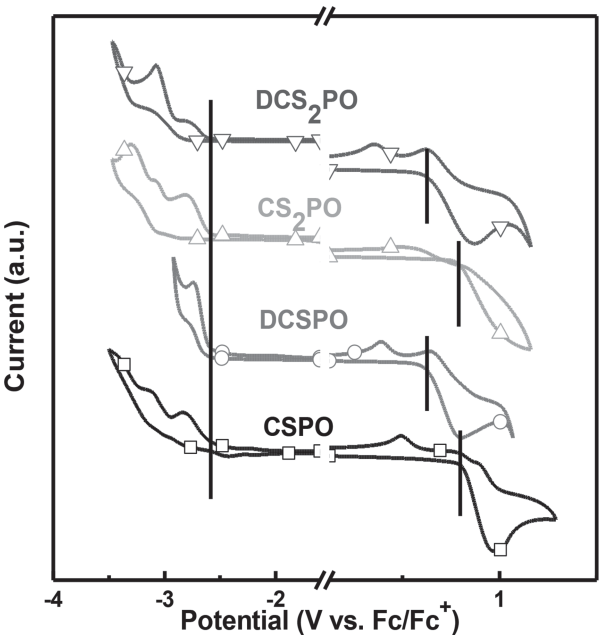

Figure 5. Cyclic voltammetry curves for CSPO, DCSPO, CS_2PO and DCS_2PO in CH_2Cl_2 for oxidation and DMF for reduction at scan rate of 100 mV s^{-1}.

2.5. Electrochemical Properties

Cyclic voltammetry (CV) was employed to investigate the electrochemical behaviours. During the cathodic scan in N,N-dimethylformamide (DMF), all these four materials possessed the similar onset reduction potentials originating from n-type PO unit (**Figure 5**). The LUMO levels were thus calculated to be –2.25, –2.19, –2.21 and –2.19 eV for CSPO, DCSPO, CS_2PO and DCS_2PO, respectively, with regard to the energy level of ferrocene (4.8 eV below vacuum). In anodic scan, CSPO and CS_2PO underwent the same oxidation processes, originating from their p-type sole carbazole unit. Thus, they exhibited similar HOMO energy levels of about –5.60 eV. For DCSPO and DCS_2PO, the p-type unit was designed as a carbazole dimer,

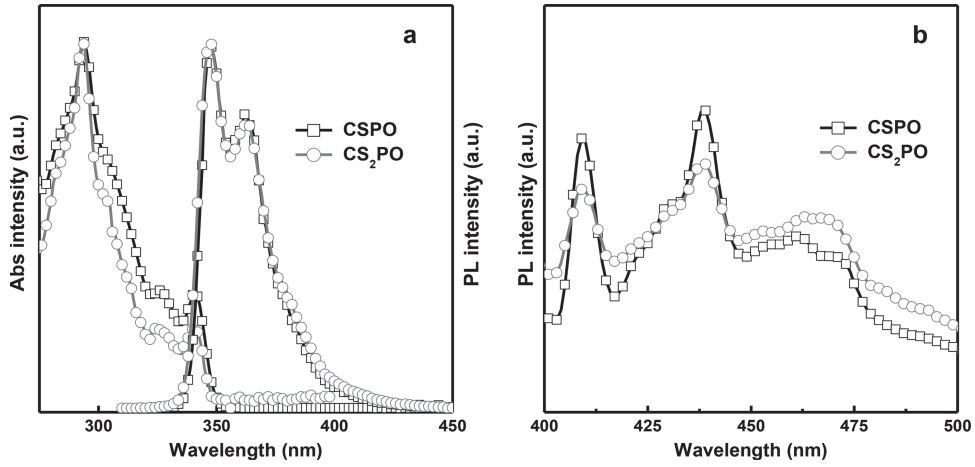

Figure 4. a) Absorption and PL spectra (excitation wavelength = 290 nm) of CSPO and CS_2PO in dilute CH_2Cl_2 (concentration = 10^{-5} M); b) PL spectra of CSPO and CS_2PO in frozen CH_2Cl_2 at 77 K (excitation wavelength = 325 nm).

Table 2. Electrochemical properties of CSPO, DCSPO, CS_2PO and DCS_2PO.

Compounds	E_{on}^{ox} [V]	HOMO [eV]	E_{on}^{red} [V]	LUMO [eV]	E_g [a)] [eV]
CSPO	0.81	−5.60	−2.57	−2.25	3.35
DCSPO	0.62	−5.43	−2.60	−2.19	3.24
CS_2PO	0.79	−5.56	−2.60	−2.21	3.35
DCS_2PO	0.63	−5.43	−2.61	−2.19	3.24

[a)]calculated according to the electrochemical result.

which made oxidation process occur more easily, resulting in higher HOMO levels of about −5.43 eV. The HOMO level of DCSPO and DCS_2PO are 0.17 eV higher than that of CSPO and CS_2PO as shown in **Table 2**. The dimer carbazole group can increase the HOMO energy level which would facilitate the hole injection in doped devices.

2.6. Theoretical Simulation

Density functional theory (DFT) calculations with the optimized geometry at B3LYP/6–31G* level were carried out to further understand their electronic properties. The distributions of the front molecular orbitals are shown in **Figure 6**. According to the DFT calculations, all the LUMO energy levels of are located on PO unit indicating the similar LUMO levels of these compounds. The HOMO energy levels are distributed on sole carbazole unit for CSPO and CS_2PO, and on the carbazole dimer for DCSPO and DCS_2PO, respectively. It is also clearly observed that the distributions of HOMO and LUMO of all the four compounds are completely separated due to the interruption effect of tetraphenylsilane. The introduction of one more silicon bridge in CS_2PO and DCS_2PO has no impact on the distribution of the frontier molecular orbitals. The intramolecular interactions between the electron-deficient PO unit and electron-donating carbazole unit are thus minimized which is favorable for the injection of electrons and holes. The theoretical calculation affords the HOMO and LUMO values in the range of −5.33 to −1.05 eV which are consistent with the CV data. The results suggest that the HOMO and LUMO energy levels can be separately modified by functional groups in tetraphenylsilane derivatives.

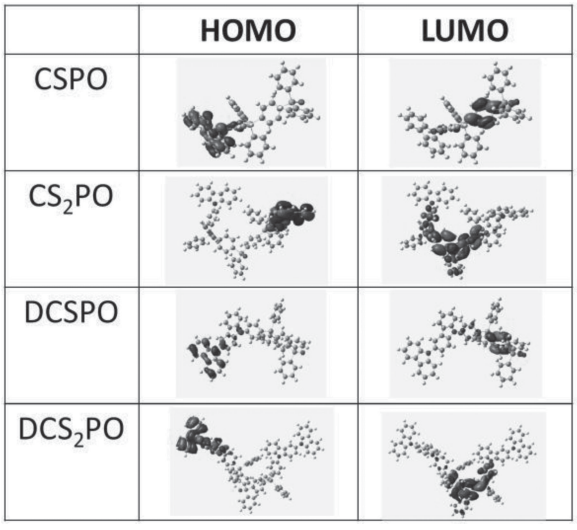

Figure 6. The distribution of HOMO and LUMO energy levels of CSPO, DCSPO, CS_2PO and DCS_2PO under B3LYP/6–31G* level.

2.7. Phosphorescent OLEDs

To evaluate the potentiality of these compounds as hosts in electroluminescent devices, the FIrpic doped spin-coating devices were fabricated with the configuration of ITO/PEDOT:PSS (40 nm)/host:FIrpic (15 wt%) (50–60 nm)/TmPyPb (5 nm)/TPBi (30 nm)/CsF (1.5 nm)/Al (120 nm). The host materials CSPO, DCSPO, CS_2PO and DCS_2PO doped with FIrpic are used as emitting layers for device A-D. All the devices show the same blue emission spectra peaking at 475 nm (**Figure 7**), which originated from the emission of FIrpic by full energy transfer form host to guest. The prominent values of (0.16, 0.33) are the typical CIE coordinates of FIrpic's emission from blue phosphorescent OLED. The data are consistent with the results published by other research groups.[9,12,15] The turn-on voltage is a little bit increase from 7.8 (Device A) to 8.6 V (Device D). Device C and D based on double-silicon bridged hosts of CS_2PO and DCS_2PO achieve much higher efficiency than that of corresponding single-silicon bridged CSPO (Device A) and DCSPO (Device B), which suggests that our design strategy takes effect in this system (**Table 3**). The introduction of double-silicon bridged center provides more stable film and better compatibility between host and guest to greatly improve the device performance. The carbazole dimer in DCS_2PO can further increase the device efficiency than that of sole carbazole unit in CS_2PO due to the better hole injection ability as revealed by electrochemistry and theoretical calculations. As a result, the device using DCS_2PO as host achieves the best performance with the maximum current efficiency of 26.5 cd A^{-1} and external quantum efficiency (EQE) of 13.6%. The device performance is comparable with those devices fabricated by solution-processable method.[10,16] Recently, Yang's group had reported highly efficient PhOLEDs based on several double-silicon centered molecules.[17] The best EL performance was achieved for the mOXDDSiPA-based blue phosphorescent device, with a maximum current efficiency of 23.4 cd A^{-1} and a maximum external quantum efficiency of 10.7%. We believe that the coupling of carbazole dimer and PO units through double-silicon bridge can also afford suitable solution-processable wide bandgap hosts for blue PhOLED.

3. Conclusion

In summary, we have developed a series of double-silicon bridged molecules as solution-processable hosts for blue phosphorescent FIrpic. The extended molecular structure in CS_2PO

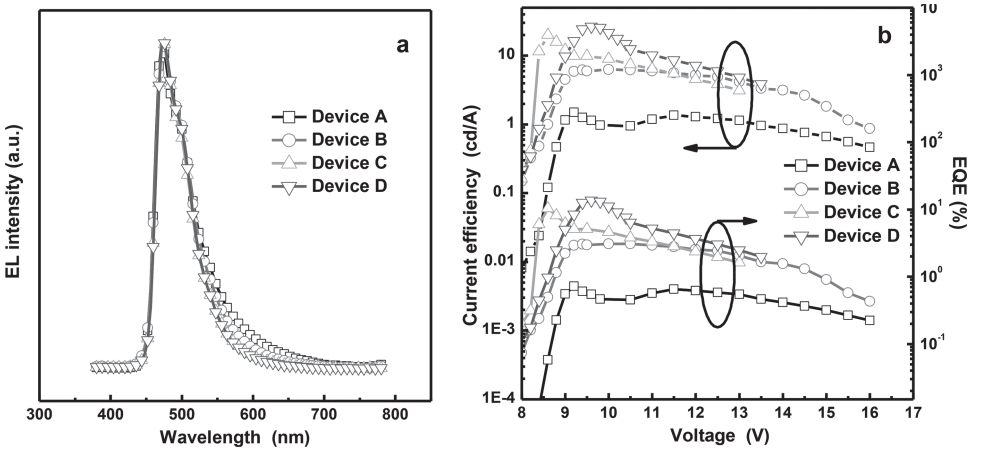

Figure 7. a) EL spectra of solution-processed doping devices A-D at 9 V; b) Current efficiency-voltage-EQE curves of solution-processed FIrpic doping devices A-D. Device structures: ITO/PEDOT:PSS (40 nm)/solution processed host:FIrpic (15 wt%) (50–60 nm)/vacuum-deposited TmPyPb (5 nm)/vacuum-deposited TPBi (30 nm)/CsF (1.5 nm)/Al (120 nm), host for Device A: CSPO (□), Device B: DCSPO (○), Device C: CS_2PO (△), Device D: DCS_2PO (▽).

and DCS_2PO improves the solution processability and thermal stability in comparison with their respective single-silicon bridged compounds of CSPO and DCSPO, without lowering their singlet and triplet energy levels. Solution-processed blue PhOLED using DCS_2PO as host achieve the best device performance. This can be attributed to its relative high triplet energy to confine triplet exciton on the guest, homogeneous morphology, appropriate energy levels to facilitate carriers injection, and more balanced carrier transporting ability in the device. These results demonstrate that the extension of molecular structure via double-silicon bridge is an effective approach to design solution-processable host materials for highly efficient blue PhOLEDs.

4. Experimental Section

4.1. Measurement

The ^1H and ^{13}C NMR spectra were recorded using a Bruker AVANCE 500 spectrometer at 500 MHz and 125 MHz respectively, at 298 K using $CDCl_3$ as the solvent and tetramethylsilane (TMS) as the internal standard. The elemental analysis was perfomed by a Flash EA 1112, CHNS-O elemental analysis instrument. The MALDI-TOF-MS mass spectra were recorded using an AXIMA-CFR^{TM} plus instrument. Thermal gravimetric analysis (TGA) was undertaken on a Perkin-Elmer thermal analysis system at a heating rate of 10 °C min^{-1} and a nitrogen flow rate of 80 ml min^{-1}. Differential scanning calorimetry (DSC) was carried out using a NETZSCH (DSC-204) instrument at 10 K min^{-1} while flushing with nitrogen. Atomic force microscopy (AFM) images were taken by tapping mode using a Nanoscope III, Digital Instrument system equipped with a 5 μm × 5 μm scanner and a silicon nitride tip with a force constant of 40 N m^{-1}. UV-vis and fluorescence spectra were recorded using a Shimadzu UV-3100 spectrophotometer and a Shimadzu RF-5301PC spectrophotometer, respectively. Electrochemical measurements were performed using a BAS 100W Bioanalytical System: a glass-carbon disk electrode was used as the working electrode, a Pt wire as the counter electrode, Ag/Ag^+ as the reference electrode and Bu_4NPF_6 (0.1 M) in N,N-dimethylformamide (DMF) or CH_2Cl_2 as the electrolyte. The pseudo-referrence electrode was calibrated externally using a 5 mM solution of ferrocene (Fc/Fc^+) in the electrolyte.

Table 3. Detailed data of spin-coating devices A-D.

Device	V_{on} [V]	CE [cd A^{-1}]	PE [lm W^{-1}]	EQE [%]	L_{max} [cd m^{-2}]	CIE [x,y]
A CSPO	7.8	1.49	0.51	0.58	333	0.17,0.34
B DCSPO	7.6	6.27	2.07	3.10	6245	0.16,0.33
C CS_2PO	8.0	20.17	7.37	10.4	2241	0.16,0.33
D DCS_2PO	8.6	26.50	8.66	13.6	4878	0.15,0.33

4.2. Device Fabrications and Measurement

Devices with configuration of ITO/PEDOT:PSS (40 nm)/host:FIrpic (15 wt%) (50–60 nm)/TmPyPb (5 nm)/TPBi (30 nm)/CsF (1.5 nm)/Al (120 nm) were fabricated as follows: PEDOT:PSS was spin-coated onto the cleaned ITO-coated substrate from its aqueous solution and then heated at 120 °C for 20 minutes to remove the residual water solvent. The emissive layer (EML) was spin-coated from chlorobezene solution with concentration of 20 mg ml^{-1}. Then the samples were annealed at 110 °C for 30 min. Finally, a hole -blocking layer of Tm3PyPB (1,3,5-tri(m-pyrid-3-yl-phenyl)benzene) (5 nm), an electron-transporting layer of TPBI (1,3,5-tri(1- phenyl-1H-benzimidazol-2-yl)benzene) (30 nm), and a cathode composed of CsF (1.5 nm) and Al (120 nm) were sequentially deposited onto the substrate by thermal evaporation at a pressure of 4.0×10^{-6} mbar. The current-voltage characteristics of the devices were measured by a Keithley 2400 sourcemeter and brightness-voltage characteristics was measured by PR650 spectroradiometer. The EQE values were calculated according to previously reported methods.[18] All the measurements were carried out at room temperature under ambient condition.

4.3. Materials

Bis(4-((4-(9-H-carbazol-9-yl)phenyl)diphenylsilyl)phenyl)(phenyl)phosphine oxide (CS_2PO): A mixture of bis(4-((4-bromophenyl)diphenylsilyl)phenyl)(phenyl)phosphine oxide (0.95 g, 1.00 mmol), carbozole (368 mg, 2.20 mmol), CuI (38 mg, 0.20 mmol), K_3PO_4 (1.06 g, 5.00 mmol), and (±)-trans-1,2-diamino-cyclohexane (280 mg, 0.20 mmol) was added to toluene (5 mL), then the mixture was refluxed under nitrogen for 24h. After cooling down, the reaction mixture was quenched with $(NH_4)_2CO_3$ solution and then extracted with CH_2Cl_2. After removal of the solvent, the residue was purified by column chromatography on silica gel using ethyl acetate/petroleum(1:2 v/v) as the eluent to give white powder

(0.83 g). Yield: 73%. ^{1}H NMR (500 MHz, $CDCl_3$, δ): 8.18 – 8.17 (4H, d, J = 7.8, Ar-H), 7.82 – 7.78 (12H, m, Ar-H), 7.73 – 7.71 (1H, d, J = 7.3, Ar-H), 7.67 – 7.64 (10H, m, Ar-H), 7.59 – 7.57 (4H, m, Ar-H), 7.53 – 7.39 (22H, m, Ar-H), 7.34 – 7.31 (4H, t, J = 7.1, J = 7.7, Ar-H). ^{13}C NMR ($CDCl_3$, 125 MHz, δ): 140.53, 139.44, 139.33, 137.89, 136.41, 133.40, 133.28, 132.97, 132.54, 132.23, 131.39, 131.31, 130.15, 129.92, 128.22, 128.04, 126.27, 125.99, 123.58, 120.35, 120.17, 109.87. Anal. calcd for $C_{78}H_{57}N_2Si_2PO$: C 83.24, H 5.10, N 2.49; found: C 82.42, H 5.24, N 2.04. MALDI-TOF m/z: $[M + H]^+$ calcd for $C_{78}H_{57}N_2Si_2PO$, 1124.37; found, 1125.30.

Bis(4-((4-(9-H-(3,9′-bicarbazol)-9-yl)phenyl)diphenylsilyl)phenyl) (phenyl)phosphine oxide (DCS2PO): The procedure for DCSPO was similar as the preparation of CS_2PO starting from 4,-dibromo-4′-diphenylphosphine oxide-tetraphenylsilane and 3-(9H-carbazol-9-yl)-9H-carbazole. Yield: 57%. ^{1}H NMR(500 MHz, $CDCl_3$, δ): 8.32 (2H, s, Ar-H), 8.23 – 8.22 (4H, d, J = 7.4, Ar-H), 8.14 – 8.13 (2H, d, J = 7.8, Ar-H), 7.89 – 7.87 (4H, d, J = 7.4, Ar-H), 7.83 – 7.79 (10H, m, Ar-H), 7.73 – 7.68 (13H, m, Ar-H), 7.60 – 7.41 (30H, m, Ar-H), 7.36 – 7.31 (6H, m, Ar-H). ^{13}C NMR (125 MHz, $CDCl_3$, δ): 141.87, 141.26, 139.67, 139.54, 139.04, 138.72, 136.42, 136.34, 134.35, 133.18, 132.87, 132.23, 132.16, 131.42, 131.35, 130.22, 130.4. 128.27, 128.06, 126.73, 126.33, 125.89 125.54, 124.62, 123.16, 120.64, 120.32, 119.66, 119.53, 110.99, 110.27, 109.82. Anal. calcd for $C_{102}H_{71}N_4OPSi_2$: C 84.15, H 4.92, N 3.85; found: C 83.76, H 5.05, N 3.58. MALDI-TOF m/z: $[M + H]^+$ calcd for $C_{102}H_{71}N_4OPSi_2$, 1455.49; found, 1456.10.

Supporting Information

Supporting Information is available from the Wiley Online Library or from the author.

Acknowledgements

This work is financially supported by the National Basic Research Program of China (973 Program, 2013CB834701, 2013CB834800), and National Science Foundation of China (Grant No. 21174050, 21374038).

Received: April 13, 2014
Revised: May 21, 2014
Published online: July 16, 2014

[1] a) H. W. Lin, S. Y. Ku, H. C. Su, C. W. Huang, Y. T. Lin, K. T. Wong, C. C. Wu, *Adv. Mater.* **2005**, *17*, 2489; b) D. Ray, K. L. Narasimhan, *Appl. Phys. Lett.* **2007**, *91*, 093516; c) S. H. Wu, W. L. Li, B. Chu, C. S. Lee, Z. S. Su, J. B. Wang, F. Yan, G. Zhang, Z. Z. Hu, Z. Q. Zhang, *Appl. Phys. Lett.* **2010**, *96*, 093302; d) G. Memisoglu, C. Varlikli, *Int. J. Photoenergy* **2012**, *55*, 1; e) C. B. Liu, M. Liu, G. B. Che, B. Su, L. Wang, X. X. Zhang, S. Zhang, *Solid State Electron.* **2013**, *89*, 68; f) L. Li, F. Zhang, Q. An, Z. Wang, J. Wang, A. Tang, H. Peng, Z. Xu, Y. Wang, *Opt. Lett.* **2013**, *38*, 3823.

[2] a) J. Dai, C. X. Xu, X. W. Sun, *Adv. Mater.* **2011**, *23*, 4284; b) Y. Zhao, A. Peng, H. Fu, Y. Ma, J. Yao, *Adv. Mater.* **2008**, *20*, 1661.

[3] a) M. Warner, S. Din, I. S. Tupitsyn, G. W. Morley, A. M. Stoneham, J. A. Gardener, Z. Wu, A. J. Fisher, S. Heutz, C. W. Kay, G. Aeppli, *Nature* **2013**, *503*, 504; b) Y. Ma, Y. Wen, J. Wang, Y. Shang, S. Du, L. Pan, G. Li, L. Yang, H. Gao, Y. Song, *J. Phys. Chem. C* **2009**, *113*, 8548.

[4] a) Y. Y. Lyu, J. Kwak, O. Kwon, S. H. Lee, D. Kim, C. Lee, K. Char, *Adv. Mater.* **2008**, *20*, 2720; b) K. H. Lee, C. S. Son, J. Y. Lee, S. Kang, K. S. Yook, S. O. Jeon, J. Y. Lee, S. S. Yoon, *Eur. J. Org. Chem.* **2011**, *25*, 4788; c) Y. J. Pu, G. Nakata, F. Satoh, H. Sasabe, D. Yokoyama, J. Kido, *Adv. Mater.* **2012**, *24*, 1765; d) H. Uoyama, K. Goushi, K. Shizu, H. Nomura, C. Adachi, *Nature* **2012**, *492*, 234; e) Q. Zhang, J. Li, K. Shizu, S. Huang, S. Hirata, H. Miyazaki, C. Adachi, *J. Am. Chem. Soc.* **2012**, *134*, 14706.

[5] a) N. Rehmann, D. Hertel, K. Meerholz, H. Becker, S. Heun, *Appl. Phys. Lett.* **2007**, *91*, 103507; b) Y. Tao, Q. Wang, C. Yang, Q. Wang, Z. Zhang, T. Zou, J. Qin, D. Ma, *Angew. Chem. Int. Ed.* **2008**, *47*, 8104; c) Y. S. Park, J. W. Kang, D. M. Kang, J. W. Park, Y. H. Kim, S. K. Kwon, J. J. Kim, *Adv. Mater.* **2008**, *20*, 1957; d) S. Reineke, F. Lindner, G. Schwartz, N. Seidler, K. Walzer, B. Lussem, K. Leo, *Nature* **2009**, *459*, 234; e) C. H. Fan, P. Sun, T. H. Su, C. H. Cheng, *Adv. Mater.* **2011**, *23*, 2981; f) T. Fleetham, J. Ecton, Z. Wang, N. Bakken, J. Li, *Adv. Mater.* **2013**, *25*, 2573.

[6] a) M. A. Baldo, D. F. O'Brien, Y. You, A. Shoustikov, S. Sibley, M. E. Thompson, S. R. Forrest, *Nature* **1998**, *395*, 151; b) Y. Ma, H. Zhang, J. Shen, C. Che, *Synth. Met.* **1998**, *94*, 245; c) M. C. G. Hernández, M. G. Zolotukhin, J. L. Maldonado, N. Rehmann, K. Meerholz, S. King, A. P. Monkman, N. Fröhlich, C. J. Kudla, U. Scherf, *Macromolecules* **2009**, *42*, 9225; d) M. C. Gather, A. Kohnen, K. Meerholz, *Adv. Mater.* **2011**, *23*, 233; e) A. Chaskar, H. F. Chen, K. T. Wong, *Adv. Mater.* **2011**, *23*, 3876; f) K. S. Yook, J. Y. Lee, *Adv. Mater.* **2012**, *24*, 3169; g) H. Sasabe, J. Kido, *J. Mater. Chem. C* **2013**, *1*, 1699.

[7] a) C. Adachi, M. A. Baldo, M. E. Thompson, S. R. Forrest, *J. Appl. Phys.* **2001**, *90*, 5048; b) D. Tanaka, H. Sasabe, Y. J. Li, S. J. Su, T. Takeda, J. Kido, *Jpn. J. Appl. Phys.* **2007**, *46*, L10; c) Z. Ma, L. Chen, J. Ding, L. Wang, X. Jing, F. Wang, *Adv. Mater.* **2011**, *23*, 3726; d) Y. C. Zhu, L. Zhou, H. Y. Li, Q. L. Xu, M. Y. Teng, Y. X. Zheng, J. L. Zuo, H. J. Zhang, X. Z. You, *Adv. Mater.* **2011**, *23*, 4041; e) M. Cai, T. Xiao, E. Hellerich, Y. Chen, R. Shinar, J. Shinar, *Adv. Mater.* **2011**, *23*, 3590; f) M. Cai, Z. Ye, T. Xiao, R. Liu, Y. Chen, R. W. Mayer, R. Biswas, K. M. Ho, R. Shinar, J. Shinar, *Adv. Mater.* **2012**, *24*, 4337; g) H. Sasabe, Y. Seino, M. Kimura, J. Kido, *Chem. Mater.* **2012**, *24*, 1404; h) H. Sasabe, H. Nakanishi, Y. Watanabe, S. Yano, M. Hirasawa, Y. J. Pu, J. Kido, *Adv. Funct. Mater.* **2013**, *23*, 5550; i) S. Lee, K. H. Kim, D. Limbach, Y. S. Park, J. J. Kim, *Adv. Funct. Mater.* **2013**, *23*, 4105.

[8] a) T. Tsuzuki, S. Tokito, *Adv.Mater.* **2007**, *19*, 276; b) H. Kim, Y. Byun, R. R. Das, B. K. Choi, P. S. Ahn, *Appl. Phys. Lett.* **2007**, *91*, 093512; c) D. H. Kim, N. S. Cho, H. Y. Oh, J. H. Yang, W. S. Jeon, J. S. Park, M. C. Suh, J. H. Kwon, *Adv. Mater.* **2011**, *23*, 2721; d) C. H. Fan, P. Sun, T. H. Su, C. H. Cheng, *Adv. Mater.* **2011**, *23*, 2981; e) T. H. Su, C. H. Fan, Y. H. Ou-Yang, L. C. Hsu, C. H. Cheng, *J. Mater. Chem. C* **2013**, *1*, 5084; f) C. H. Lin, C. W. Hsu, J. L. Liao, Y. M. Cheng, Y. Chi, T. Y. Lin, M. W. Chung, P. T. Chou, G. H. Lee, C. H. Chang, C. Y. Shih, C. L. Ho, *J. Mater. Chem.* **2012**, *22*, 10684.

[9] a) S. J. Su, E. Gonmori, H. Sasabe, J. Kido, *Adv. Mater.* **2008**, *20*, 4189; b) L. Xiao, S. J. Su, Y. Agata, H. Lan, J. Kido, *Adv. Mater.* **2009**, *21*, 1271; c) H. H. Chou, C. H. Cheng, *Adv. Mater.* **2010**, *22*, 2468; d) J. S. Swensen, E. Polikarpov, A. Von Ruden, L. Wang, L. S. Sapochak, A. B. Padmaperuma, *Adv. Funct. Mater.* **2011**, *21*, 3250; e) C. Han, Z. Zhang, H. Xu, S. Yue, J. Li, P. Yan, Z. Deng, Y. Zhao, P. Yan, S. Liu, *J. Am. Chem. Soc.* **2012**, *134*, 19179; f) X. Yang, H. Huang, B. Pan, M. P. Aldred, S. Zhuang, L. Wang, J. Chen, D. Ma, *J. Phys. Chem. C* **2012**, *116*, 15041; g) Y. H. Son, Y. J. Kim, M. J. Park, H.-Y. Oh, J. S. Park, J. H. Yang, M. C. Suh, J. H. Kwon, *J. Mater. Chem. C* **2013**, *1*, 5008; h) C. W. Lee, J. Y. Lee, *Adv. Mater.* **2013**, *25*, 5450.

[10] a) H. Wu, L. Ying, W. Yang, Y. Cao, *Chem. Soc. Rev.* **2009**, *38*, 3391; b) E. Ahmed, T. Earmme, S. A. Jenekhe, *Adv. Funct. Mater.* **2011**, *21*, 3889; c) M. C. Gather, A. Kohnen, K. Meerholz, *Adv. Mater.* **2011**, *23*, 233.

[11] a) X. H. Zhou, Y. H. Niu, F. Huang, M. S. Liu, A. K. Y. Jen, *Macromolecules* **2007**, *40*, 3015; b) D. Hu, G. Cheng, P. Lu, H. Liu, F. Shen, F. Li, Y. Lv, W. Dong, Y. Ma, *Macromol. Rapid Comm.* **2011**, *32*, 1467.
[12] a) X. Ren, J. Li, R. J. Holmes, P. I. Djurovich, S. R. Forrest, M. E. Thompson, *Chem. Mater.* **2004**, *16*, 4743; b) S. J. Yeh, M. F. Wu, C. T. Chen, Y. H. Song, Y. Chi, M. H. Ho, S. F. Hsu, C. H. Chen, *Adv. Mater.* **2005**, *17*, 285; c) J. K. Bin, N. S. Cho, J. I. Hong, *Adv. Mater.* **2012**, *24*, 2911.
[13] a) S. Gong, Q. Fu, Q. Wang, C. Yang, C. Zhong, J. Qin, D. Ma, *Adv. Mater.* **2011**, *23*, 4956; b) S. Gong, Y. Chen, J. Luo, C. Yang, C. Zhong, J. Qin, D. Ma, *Adv. Funct. Mater.* **2011**, *21*, 1168.
[14] H. Liu, G. Cheng, D. Hu, F. Shen, Y. Lv, G. Sun, B. Yang, P. Lu, Y. Ma, *Adv. Funct. Mater.* **2012**, *22*, 2830.
[15] M. H. Tsai, T. H. Ke, H. W. Lin, C. C. Wu, S. F. Chiu, F. C. Fang, Y. L. Liao, K. T. Wong, Y. H. Chen, C. I. Wu, *Appl. Mater. Inter.* **2009**, *1*, 567.
[16] a) K. S. Yook, S. E. Jang, S. O. Jeon, J. Y. Lee, *Adv. Mater.* **2010**, *22*, 4479; b) S. Shao, J. Ding, T. Ye, Z. Xie, L. Wang, X. Jing, F. Wang, *Adv. Mater.* **2011**, *23*, 3570; c) T. Earmme, S. A. Jenekhe, *Adv. Mater.* **2012**, *22*, 5126.
[17] a) S. Gong, Q. Fu, W. Zeng, C. Zhong, C. Yang, D. Ma, J. Qin, *Chem. Mater.* **2012**, *24*, 3120; b) S. Gong, C. Zhong, Q. Fu, D. Ma, J. Qin, C. Yang, *J. Phys. Chem. C* **2013**, *117*, 549.
[18] S. Okamoto, K. Tanaka, Y. Izumi, H. Adachi, T. Yamiji, T. Suzuki, *Jpn. J. Appl. Phys.* **2001**, *40*, 783.